

NASA TECHNICAL NOTE



NASA TN D-5298

NASA TN D-5298

FLIGHT INVESTIGATION OF A FLUIDIC AUTOPILOT SYSTEM

by Wilton P. Lock and Shu W. Gee

Flight Research Center

Edwards, Calif.

NATIONAL AERONAUTICS AND SPACE ADMINISTRATION • WASHINGTON, D. C. • JULY 1969

FLIGHT INVESTIGATION OF A FLUIDIC AUTOPILOT SYSTEM

By Wilton P. Lock and Shu W. Gee

Flight Research Center
Edwards, Calif.

NATIONAL AERONAUTICS AND SPACE ADMINISTRATION

For sale by the Clearinghouse for Federal Scientific and Technical Information
Springfield, Virginia 22151 - CFSTI price \$3.00

FLIGHT INVESTIGATION OF A FLUIDIC AUTOPILOT SYSTEM

By Wilton P. Lock and Shu W. Gee
Flight Research Center

SUMMARY

A flight investigation was made of an experimental fluidic flight control system capable of various modes of operation, including altitude hold, heading hold, wings leveler, and turn control. The fluidic control system was tested in each mode at two flight conditions: cruise at 5000 feet, and cruise at 10,000 feet.

Although stability problems were encountered early in the program, stable performance was achieved in each control mode for the flight conditions tested. High reliability was demonstrated, in that there were no failures with the fluidic elements themselves. Failures were experienced, however, with the mechanical portion of the mechanical fluidic components.

Flight investigation revealed a number of areas in which improvement is needed before the system can be considered operational. Aircraft altitude changes caused noticeable changes in the null of the fluidic components, and gain reduction with increased altitude was experienced with sensors and amplifiers.

INTRODUCTION

Anticipating a potential application of fluidic systems in future aerospace design, the NASA Flight Research Center undertook a program to develop a fluidic flight control system for a small general aviation type of aircraft and to investigate the capabilities of the system in routine day-to-day operations. The program sought not only to provide operational experience with a fluidic system but also to verify system performance and predicted high reliability. Additional goals of the program were to develop fluid control functions to aid pilots of light aircraft under adverse flying conditions and to provide a system test-bed to investigate additional control functions.

The program began with a feasibility study contract with Honeywell Inc., of Minneapolis, Minn., to investigate the various concepts suitable for fluid mechanization of a flight-path control system (ref. 1). This contract was followed with a contract amendment for Honeywell to design, develop, and fabricate a fluidic flight control system capable of providing a wings-leveler mode, a heading-hold mode, and an altitude-hold mode.

This system was subsequently installed in an Aero Commander aircraft and subjected to a series of in-flight developmental tests. The results of these tests (refs. 2

and 3) revealed an unstable altitude-hold mode. In general, altitude-hold control was found to be more difficult and problematical to mechanize than roll control. Therefore, a greater effort was placed on the control-loop design of the pitch axis. Thirty flights extending over one year were required to complete the program. This paper presents the results of the flight tests and describes the system mechanization. Details of the flight evaluation and operational problems encountered are included. No attempt is made to compare the performance of the fluidic system with the theoretical model or other types of systems. The theoretical model was known to be in error because the limited information concerning the characteristics of the aircraft and the assumptions made contributed to inaccuracies in the data used in the design phase, as described in reference 2. To compare performance with other production types of general aviation autopilot systems was considered premature because of the relative development between the fluidic and other production systems.

SYMBOLS

G	loop gain
$G_{\delta a_r}$	wings-leveler gain, $\frac{\text{deg}}{\text{deg/sec}}$
$G_{\delta a_\psi}$	heading gain, $\frac{\text{deg}}{\text{deg}}$
$G_{\delta e_q}$	pitch-rate gain, $\frac{\text{deg}}{\text{deg/sec}}$
$G_{\delta e_{\Delta h}}$	altitude gain, $\frac{\text{deg}}{\text{ft}}$
$G_{\delta r_r}$	yaw-rate gain, $\frac{\text{deg}}{\text{deg/sec}}$
K	transfer-function constant
q	pitch rate, deg/sec
r	yaw rate, deg/sec

s	Laplace operator
t	time, sec
Δh	altitude error, ft
Δp	differential pressure, psig
δ_a	aileron-surface deflection, deg
δ_e	elevator-surface deflection, deg
δ_r	rudder-surface deflection, deg
θ	pitch attitude, deg
τ	time constant, sec
φ	roll-attitude angle, deg
ψ_{ac}	aircraft heading, deg
ψ_c	heading command, deg

TEST AIRPLANE

The fluidic control system was designed specifically for an Aero Commander 680 FP airplane operated by the NASA Flight Research Center. The test airplane is a seven-place, high-wing, twin-engine, general aviation airplane with a pressurized cabin. The physical characteristics are presented in the following table.

Powerplant	2 Lycoming engines
Takeoff power per engine, brake horse power	380
Maximum continuous power per engine, brake horse power	360
Empty weight (approximate), pounds	4800
Gross weight, pounds	8000
Overall length, feet	35.10
Height to top of vertical tail, feet	14.50
Wing span, feet	49.04
Wing area, square feet	255

A photograph of the airplane is shown in figure 1. The vehicle cruises at a maximum indicated airspeed of 200 knots at sea level. The basic control system consists of a wheel and pedals connected to the surfaces by cables; this is a reversible type of system in that control-surface motion causes motion of the pilot's controls.

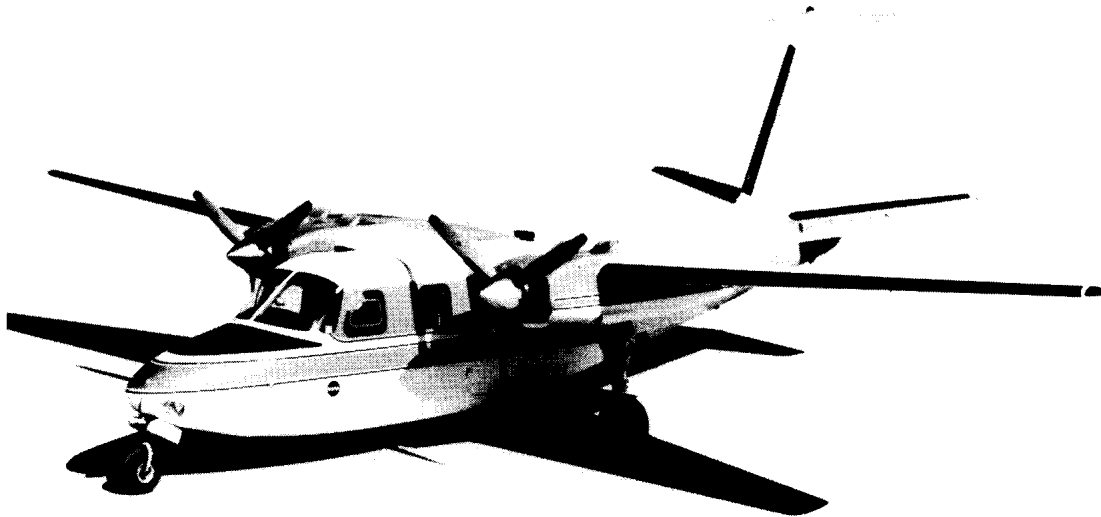


Figure 1.—NASA Aero Commander airplane.

SYSTEM DESCRIPTION

The fluidic control system is an autopilot system that can perform piloting tasks such as holding the aircraft in a steady turn, holding a desired heading, holding altitude, or maintaining a wings-level attitude. These tasks, or modes of operation, can be initiated by the pilot selecting the desired mode on a function-selector panel. The function-selector switches on the panel provide ON-OFF for master power, roll-yaw, heading-hold, and altitude-hold modes of operation. Additionally, a turn-control knob is provided for turns, and trim controls are provided to eliminate switching transients when the system is first engaged. The characteristics and principles of operation of the various sensors, amplifiers, shaping networks, and actuators used in the mechanization of this fluidic control system are described in the appendix.

Lateral-Directional Control System

Originally, the lateral-axis control system was to be a basic "wings leveler" which used yaw-rate feedback to the ailerons. Similarly, the heading-hold mode used

heading-error feedback to the ailerons. The adverse aileron yaw characteristics of the Aero Commander, however, caused the heading-hold mode to become unstable and necessitated the addition of a rudder control. Analog simulation indicated that the addition of yaw-rate feedback to the rudder control would result in a stable system. This feature was subsequently added to the basic system.

A block diagram of the lateral-directional control system is shown in figure 2.

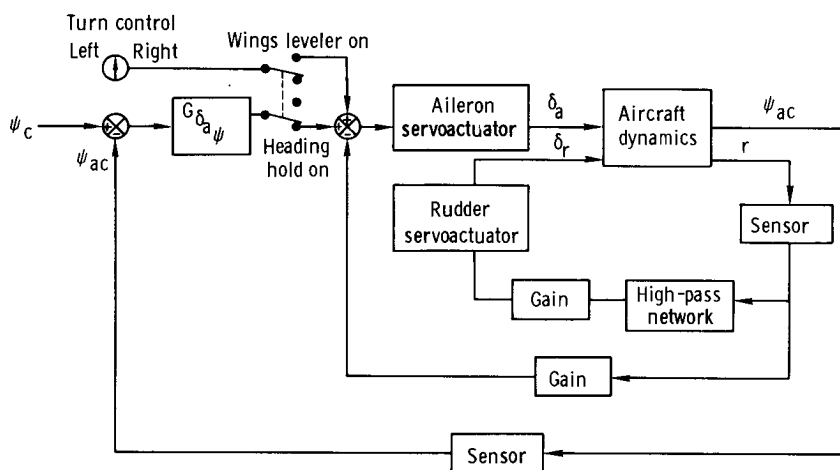


Figure 2.—Block diagram of the lateral-directional control system.

A vortex rate sensor is used for both yaw damping and wings leveling. In the yaw-damping mode, a high-pass network, approximated by the transfer function $\frac{2s}{2s + 1}$, is required to maintain vehicle maneuverability. Each loop gain was adjusted to a specified value prior to flight.

The wings-leveler mode is a control loop in the lateral axis which brings the aircraft to a wings-level attitude when the controls are released by the pilot. Yaw rate is sensed and fed to the aileron control to reduce the yaw rate to zero; the result is essentially wings-level flight. It is of interest to note that wings-level attitude is achieved without the use of an attitude reference sensor.

The heading-hold mode steers the aircraft to any heading commanded by the pilot. The error between commanded heading and the directional gyro is fed to the aileron control. System constraints provided by the gyro-error pickoff limit the selected heading to within 90° of the previous heading; for example, a 120° heading change may be accomplished by an initial command of 80° and then a final command for the remaining 40°.

A turn control permits the pilot to command continuous turn rates from 0 degrees per second to 3 degrees per second. The system is mechanized so that the selection of the heading-hold mode disengages this turn control.

Longitudinal Control System

A block diagram of the altitude-hold mode is shown in figure 3. This mode causes the aircraft to maintain pressure altitude when the system is engaged. The stabilizing loop for the altitude-hold mode is the pitch damper. Two sensors are shown in the figure, one to measure aircraft pitch rate, and the other to measure altitude error. The altitude-error signal is shaped by a lead-lag network and then summed with the pitch-rate signal. The system loop gain is variable but can only be adjusted prior to flight.

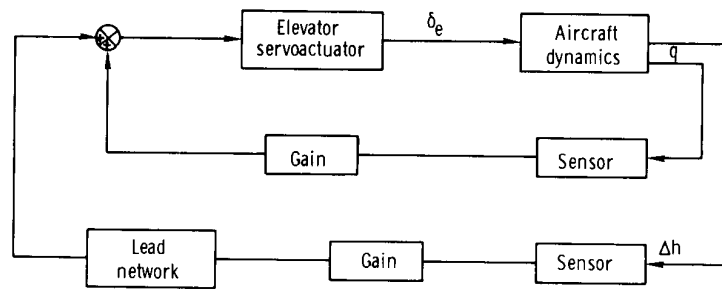


Figure 3. - Block diagram of the longitudinal control system.

Actuator and Power Systems

Modified off-the-shelf pneumatic actuators were used to satisfy the servo requirements. These actuators were connected in parallel with the basic aircraft control system, thus enabling the pilot to be aware at all times of control-system inputs.

The actuator output force is limited so that the pilot may override the fluidic control system at any time with a control-wheel pressure of 15 pounds in pitch and roll and a rudder-pedal force of 30 pounds in yaw.

The fluidic system shares a common power source with the aircraft flight instruments and the de-icer system. A schematic drawing of the Aero Commander pneumatic system and fluidic control system is shown in figure 4. Operation of the de-icer and fluid systems is controlled by solenoid valves so that either system may be operated singly but not simultaneously. When both systems are off, the de-icer regulator opens and allows air to be dumped overboard.

When the regulator-separator valve is closed, the supply pressure is 17.5 psig. For fluidic-system operation, this air supply is routed to the pressure manifold where the airflow is distributed to two precision regulators and three power amplifiers. The regulators are set at 1.5 psig and 4 psig, as illustrated, for operation of the various fluid components, such as the vortex rate sensors, amplifiers, function selector, direction gyro, and altitude sensor. The pressure drop through the valves, regulators, and manifold results in a maximum available supply pressure of 13.5 psig for the power amplifiers.

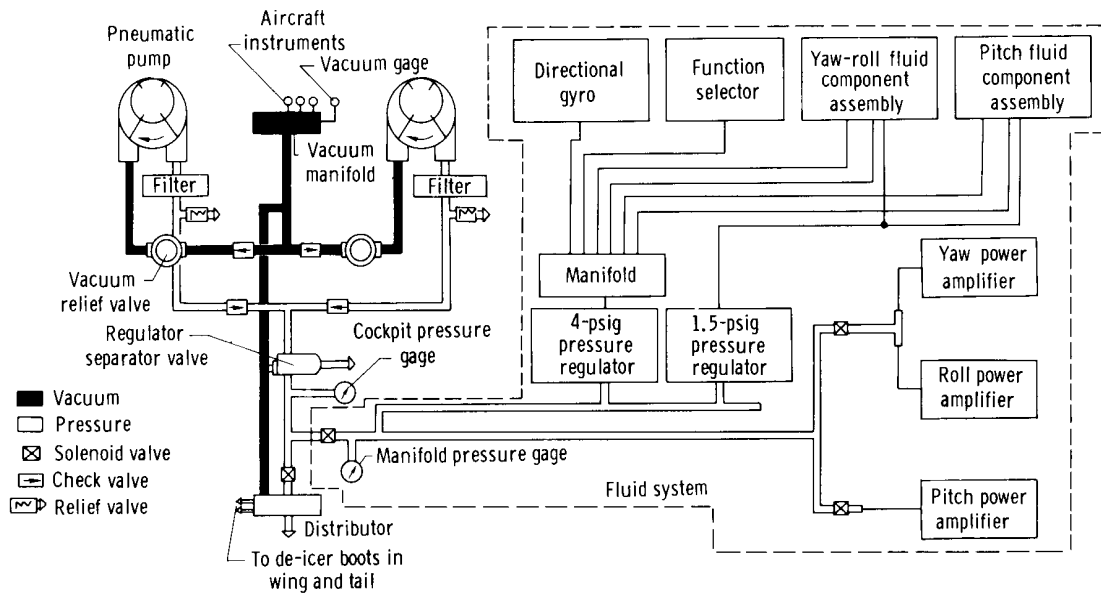


Figure 4. -Schematic drawing of the Aero Commander pneumatic system and fluidic control system.

Figure 5 is a photograph of the packaged fluidic control system components. All sensing elements except the directional gyro are packaged in the respective fluidic

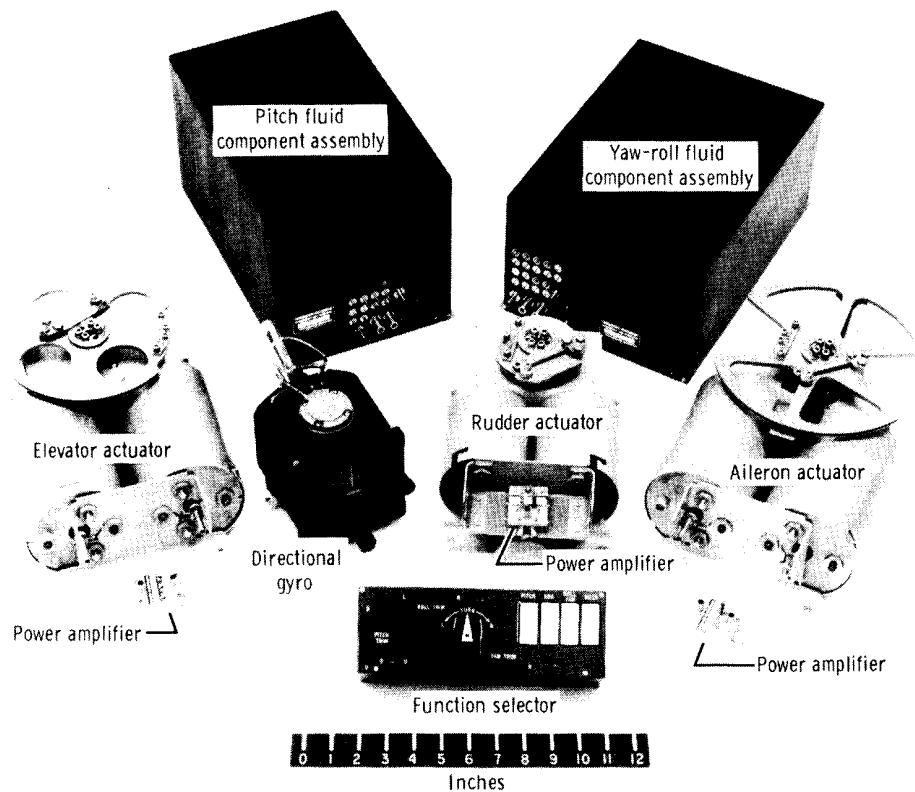


Figure 5.-Fluidic system components.

E-14671

component assembly. The relative locations of the major components in the Aero Commander are shown in figure 6.

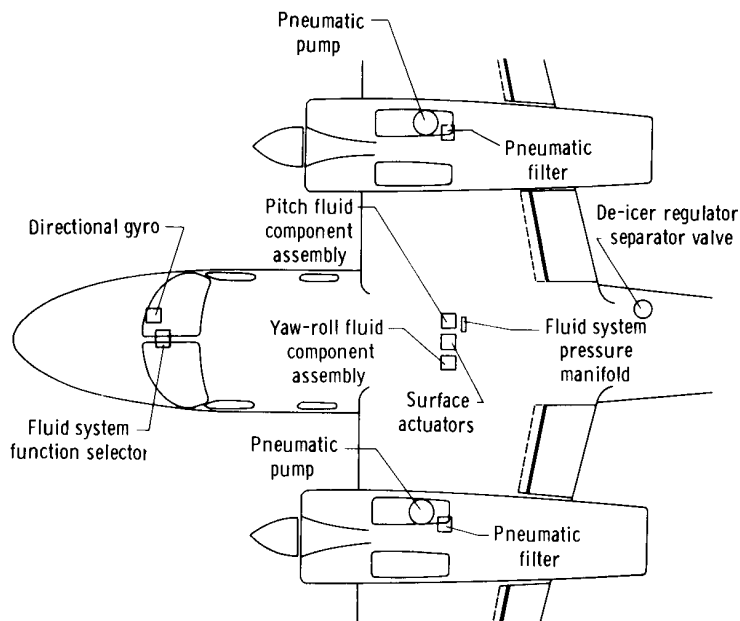


Figure 6.--Location of fluidic system components in the Aero Commander.

Because of the lack of available space in the cabin of the test aircraft, the function selector was mounted in the map case between the pilot and copilot seats approximately 8 inches above the cabin floor. The directional gyro was mounted in the right-hand panel, and the remaining fluidic components were on the forward wall of the baggage compartment.

INSTRUMENTATION

To monitor the performance of the fluidic system, an instrumentation package was fabricated to fit the cabin seat mounting rails of the Aero Commander. The package contained an 8-channel oscillograph flight recorder, one vertical gyroscope, three rate gyroscopes, one normal accelerometer, one self-balancing thermocouple readout, and three pressure-transducer amplifiers. Potentiometers were installed in the aircraft to measure the surface position of the aileron, elevator, and rudder. Twelve parameters were available for recording; however, only eight could be recorded at any one time.

FLIGHT EVALUATION

The data presented in this paper were taken from two cruise-flight conditions: 160 knots indicated airspeed (KIAS) at 5000 feet altitude using 2600 rpm, and 160 KIAS at 10,000 feet altitude using 2800 rpm. Flights were made in both smooth air and moderately turbulent air. Each of the basic modes was evaluated.

Wings-Leveler Mode

The wings-leveler mode was first flown intentionally with less than the calculated nominal gain value for the yaw-rate-to-aileron and the yaw-rate-to-rudder feedbacks. These values corresponded to pressure gains of 375 and 390 for the aileron and rudder loops, respectively, which were verified to be lower than desired. The yaw-rate-to-aileron pressure gain was later tested in flight at 544, which was considered satisfactory. The yaw-rate-to-rudder pressure gain was also increased on successive flights to 900, with satisfactory results. Pressure gain is the ratio of the pressure differential measured across the actuator (output) with respect to the pressure differential measured across the corresponding sensor (input) in units of psi/psi. The pressure gain is used for convenience, since actual system gain varies with altitude. The relationship of pressure gain to system gain at various altitudes is shown in the following table:

Loop gain	Pressure gain, psi/psi	System gain at an altitude of -		
		2,000 ft	5,000 ft	10,000 ft
$G_{\delta_{a_r}}$	375	0.690	0.660	0.615
	544	1.000	.957	.892
$G_{\delta_{r_r}}$	390	.314	.300	.280
	900	.724	.693	.646
$G_{\delta_{e_q}}$	590	.407	.389	.363
	1100	.759	.726	.676
$G_{\delta_{e_{\Delta h}}}$	170	.026	.024	.020
	36	.006	.005	.004

The performance of the wings-leveler mode with the final gain selections is shown in figure 7 for $\pm 30^\circ$ bank-angle initial conditions. The data were obtained at an altitude

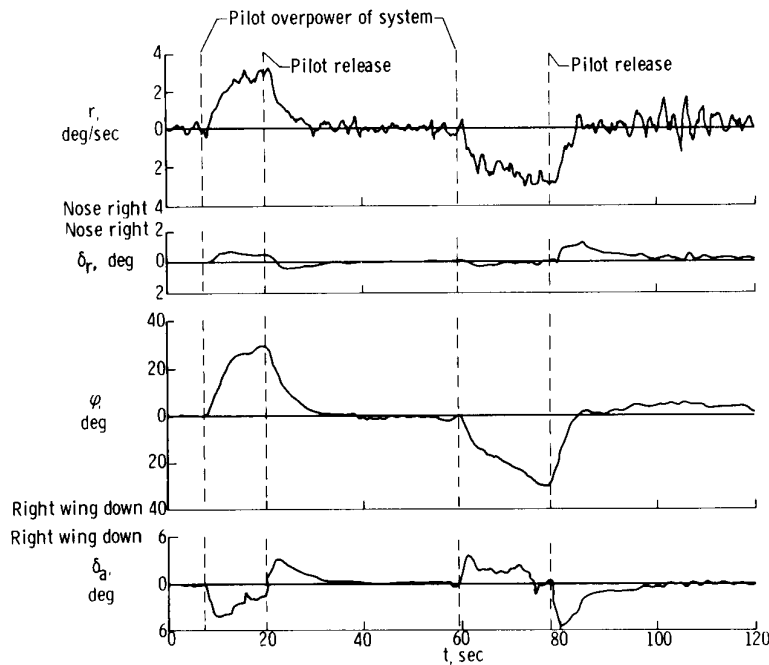


Figure 7.—Response of the Aero Commander airplane to initial conditions of 30° bank angle at 5000 feet altitude and 160 KIAS with wings-leveler mode engaged.

of 5000 feet and 160 KIAS. The wings-leveler mode was engaged in a wings-level attitude, and the pilot overpowered the system to establish an initial bank angle of 30° to the left. The controls were then released, and the aircraft response was observed. As shown, the system returned the aircraft to essentially a wings-level condition in approximately 10 seconds. When repeated for a 30° right bank, the maneuver resulted in a nearly identical response.

The response to $\pm 30^\circ$ bank-angle initial conditions was also investigated at an altitude of 10,000 feet, 160 KIAS, and 2800 rpm. Figure 8 shows that the aircraft, when released from a left-bank condition, took approximately 25 seconds to reach a wings-level position, followed by a 2° constant overshoot. The pilot returned the aircraft to a wings-level condition, and the maneuver was repeated for a 30° right bank. When released, the airplane required only 14 seconds to obtain a wings-level condition followed by an 8° overshoot which gradually decreased to about a 5° offset.

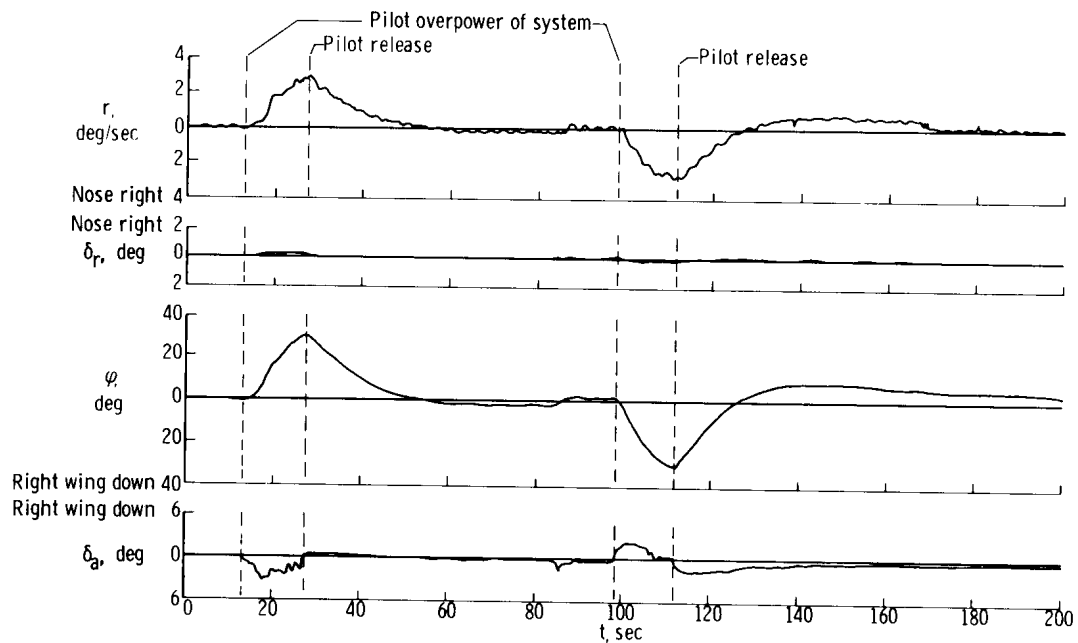


Figure 8.—Response of the Aero Commander airplane to initial conditions of 30° bank angle at 10,000 feet altitude and 160 KIAS with wings-leveler mode engaged.

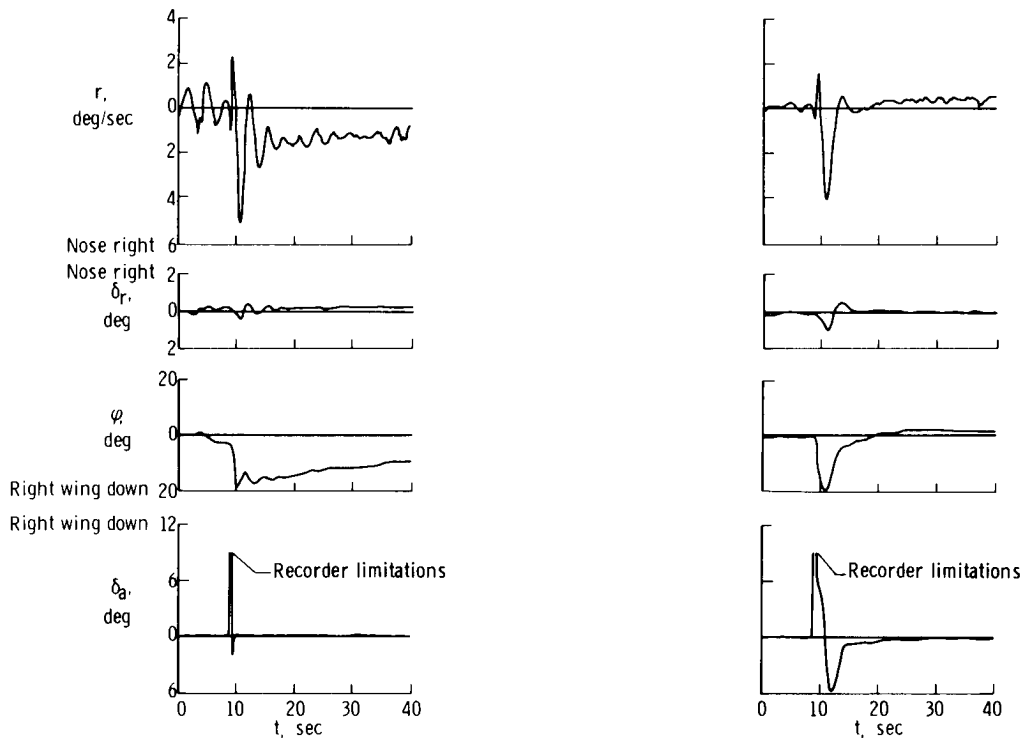
The difference in bank-angle overshoot for the two successive maneuvers at a given flight condition was attributed partly to trim changes in the fluidic system during the maneuvers. The out-of-trim condition was particularly noticeable when the maneuver was performed during the absence of turbulence, and the magnitude of mistrim was generally larger at the higher altitude test condition.

The difference in system response between the two flight altitudes was caused primarily by the reduction in system gain with increased altitude. This is shown by the bank-angle restoring rate for the different altitudes tested. The system response at 5000 feet caused a maximum roll rate of about 5.8 degrees per second, whereas at

10,000 feet the maximum rate was reduced to 2 degrees per second. The reduction in system gain with increased altitude was at first believed to result from the characteristics of the vortex rate sensor. For a given supply pressure, the gain of the vortex rate sensor was directly proportional to the mass flow of the fluid through the sensor. The temperature changes with altitude had little effect on the mass flow, and, since the supply pressure remained essentially constant, the mass-flow changes must have been caused by air-density changes. Further checks also confirmed a gain reduction with increased altitude in the first three amplifier stages.

During the overpower maneuvers for both test conditions, a small amount of rudder displacement was obtained through the yaw-damper loop of the system. This would indicate that some of the signal was passing through the high-pass network and that the network was not functioning as designed. However, the pilot did not consider this to be objectionable, but additional work on the shaping network would be necessary to correct the problem. The gain reduction with increase in altitude is shown by the rudder displacement, which is less at 10,000 feet than at 5000 feet for a similar yaw rate.

A comparison of aircraft response to a right aileron pulse without and with the wings-leveler mode engaged is shown in figure 9. The maneuver was performed at 5000 feet altitude. The free-aircraft response exhibited the usual short-period oscillation and a near neutrally stable spiral mode. The maneuver performed with the system engaged indicated that the short-period mode had improved damping and spiral characteristics. Similar results were obtained from a left aileron pulse.

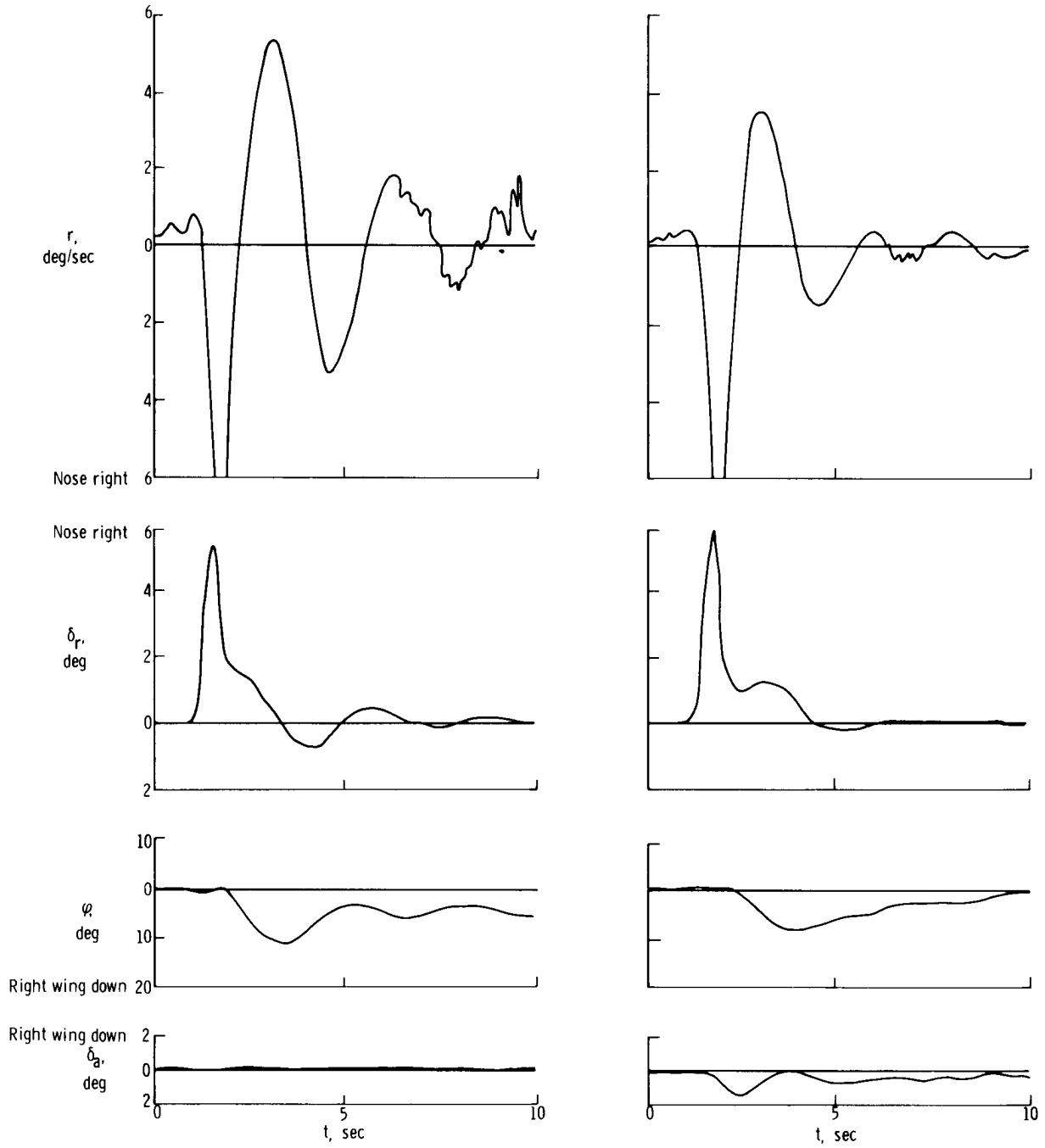


(a) Basic aircraft only.

(b) Aircraft with wings-leveler mode engaged.

Figure 9.—Response of the Aero Commander airplane to an aileron pulse at 5000 feet altitude.

Figure 10 compares aircraft response to a nose-right rudder pulse without and with the wings-leveler mode engaged at 5000 feet altitude. The damping ratio was increased from 0.18 to 0.30 after the wings-leveler mode was engaged.

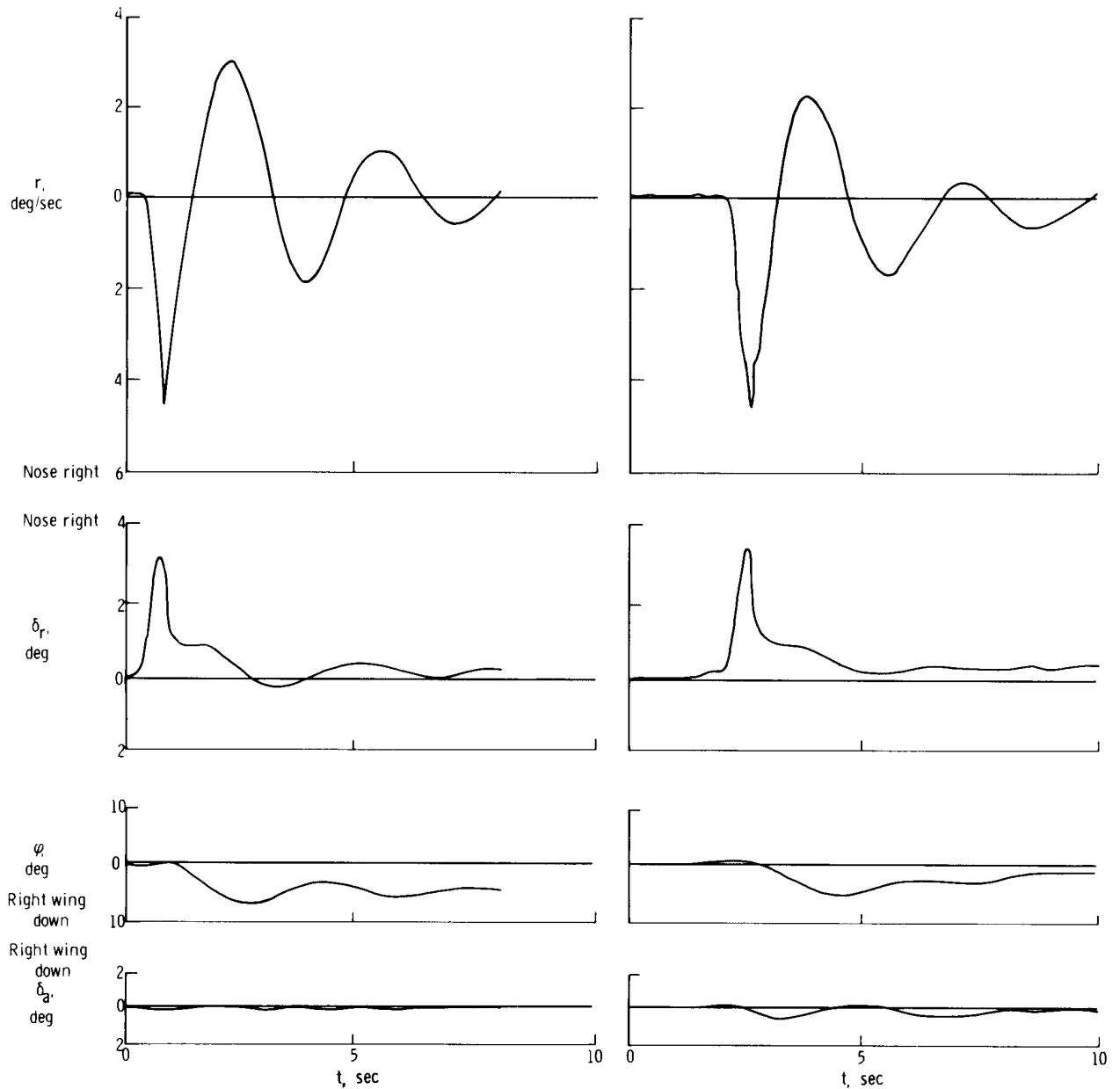


(a) Basic aircraft only.

(b) Aircraft with the wings-leveler mode engaged.

Figure 10.—Response of the Aero Commander airplane to a rudder pulse at 5000 feet altitude.

Figure 11 shows the same test at 10,000 feet altitude. The damping ratio is 0.16 for the basic airplane and 0.20 for the augmented airplane; as expected, the damping ratio for the augmented airplane was less than that measured at 5000 feet altitude, but was somewhat better than the damping ratio of the basic airplane.



(a) Basic aircraft only.

(b) Aircraft with the wings-leveler mode engaged.

Figure 11.—Response of the Aero Commander airplane to a rudder pulse at 10,000 feet altitude.

Turn-Control Mode

To investigate system performance in the turn-control mode, the turn-control gain was adjusted for ± 3 degrees per second turn rate for end-to-end mechanical travel of the turn-control knob.

Figure 12 shows a commanded right turn using the turn-control feature of the fluidic control system at 5000 feet altitude. After the pilot commanded the turn, the aircraft rolled into a right bank of about 22° and developed a steady yaw rate of almost 3 degrees per second until a recovery was commanded. The recovery from the turn was smooth, and the aircraft returned to a wings-level attitude.

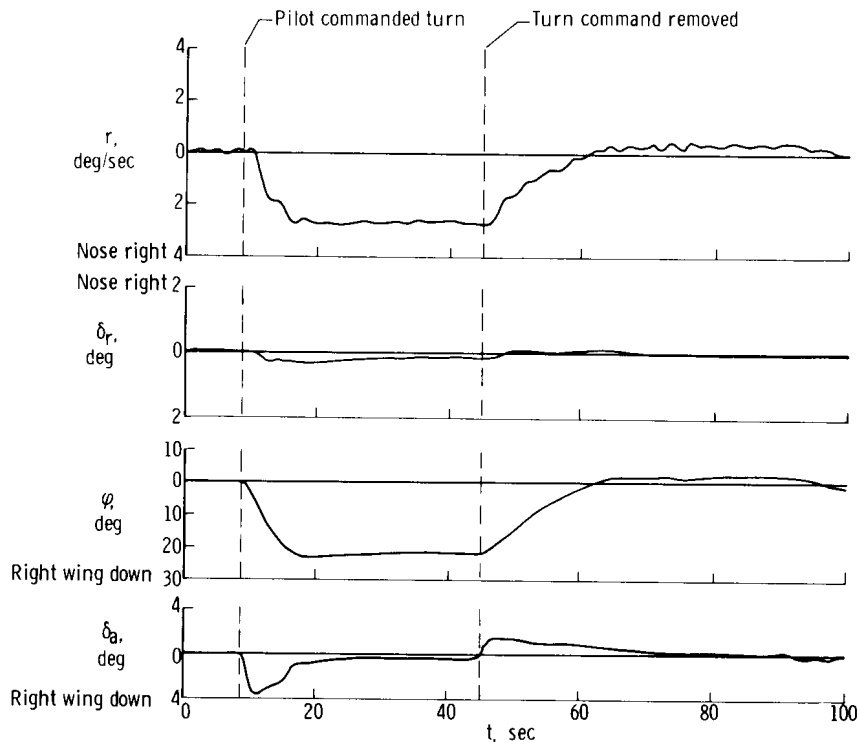


Figure 12.—Turn-control performance of the Aero Commander airplane with the turn-control mode engaged at 5000 feet altitude.

The performance of a commanded right turn at 10,000 feet altitude in which the pilot did not demand full system authority is shown in figure 13. The system provided a turn rate of 1.5 degrees per second and a bank angle of 16° . Rollout was smooth, with a constant 3° roll-attitude overshoot. Here again a trim error prevented the system from returning the aircraft to a wings-level attitude.

Figures 12 and 13 also show some rudder movement contributed by the yaw-damper loop, which indicated that the high-pass network was not functioning as expected. However, the overall performance of the turn-control mode was considered to be satisfactory.

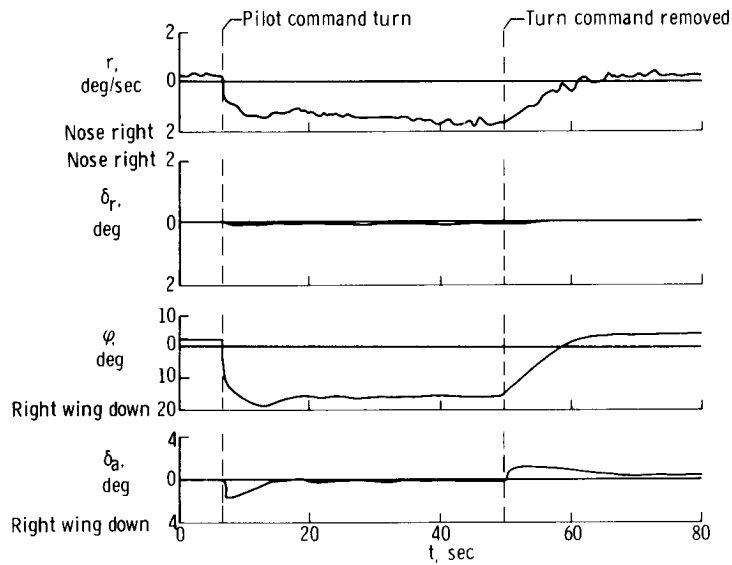


Figure 13.—Turn control performance of the Aero Commander airplane with the turn-control mode engaged at 10,000 feet altitude.

Heading-Hold Mode

For the heading-hold mode to function, the wings-leveler mode must be engaged. The performance of the heading-hold mode at 10,000 feet altitude is shown in figure 14.

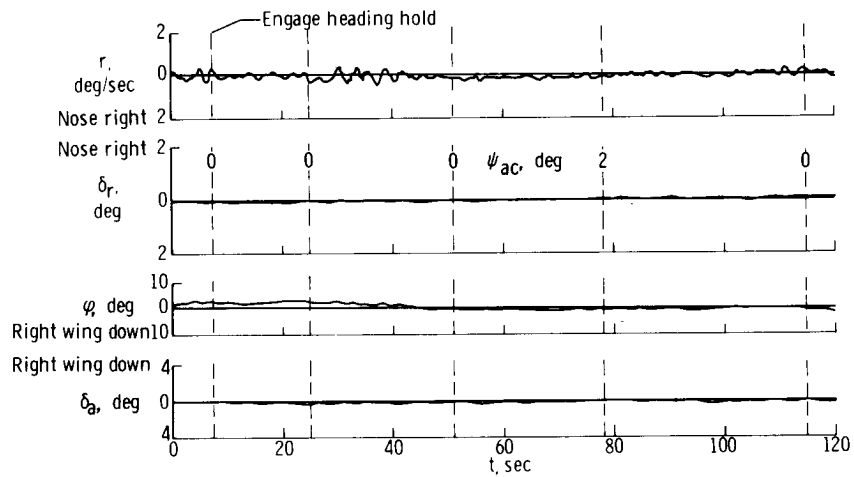


Figure 14.—Heading-hold-mode performance of the fluidic system in the Aero Commander airplane at 10,000 feet altitude.

The gyro heading and heading command were both set to zero just before the heading-hold mode was engaged. Aircraft heading as read by the pilot is shown on the yaw-rate plot. The figure shows only the first 2 minutes of data taken for a heading-hold-mode test which lasted approximately 17 minutes. During the 2-minute interval shown, the maximum heading error was only 2° ; at the end of 4.5 minutes of flight the pilot reported observing an error of $\pm 3^\circ$. Over the last half of this test, the aircraft was flying in light-to-moderate turbulence. Although heading deviations of approximately $\pm 12^\circ$ were observed during the heavier turbulence portion of the flight, the heading deviation reported by the pilot just before the system was disengaged was $\pm 6^\circ$.

The results of a commanded heading change at 5000 feet altitude are shown in figure 15. The heading-hold mode was engaged when the aircraft heading was 092° . The heading-select knob was reset to command a heading change to 180° . The aircraft initiated a right bank to establish the new heading. The system produced a 6° overshoot and gradually settled out to the selected heading. Heading callouts are again recorded on the time history for reference. The excursions about the wings-level attitude were caused by atmospheric turbulence.

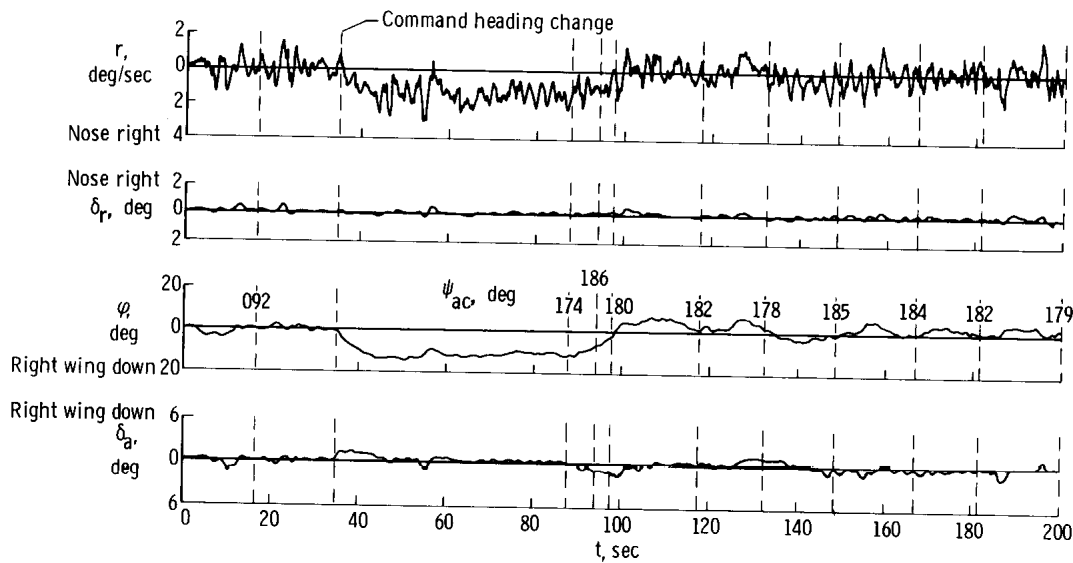


Figure 15.—Heading-hold-mode performance of the fluidic system in the Aero Commander airplane at 5000 feet altitude for a commanded heading change of 88° .

Figure 16 is a time history of the heading-hold performance at 10,000 feet altitude for a commanded heading change of 25° . The system provided the correct input for the heading change, and, as a result of a more accurate trim condition, the aircraft settled on the desired new heading. Slower response is observed in this time history than in figure 15. This is again attributed to a loss in overall system gain with increase in altitude.

Additional work needs to be done to improve the performance of this mode of control. In particular, the directional gyro used in the mechanization of the heading-hold loop has several undesirable characteristics, such as unsymmetrical output and a short linear range. These characteristics along with those of other components are described in detail in reference 2.

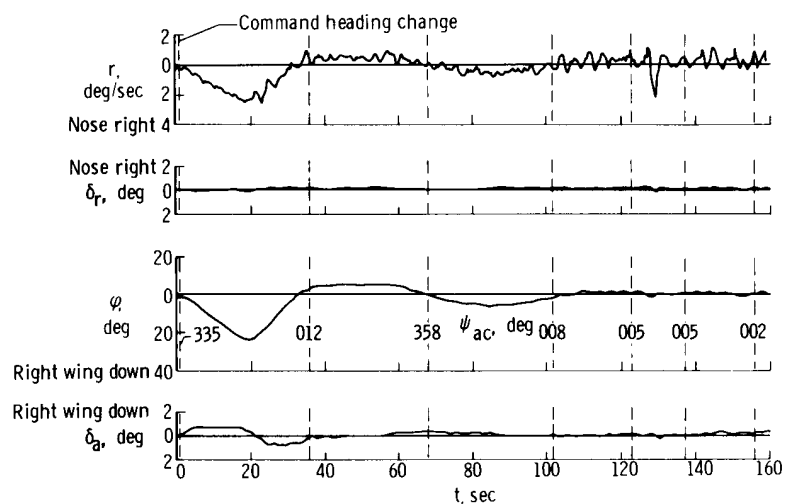


Figure 16.—Heading-hold-mode performance of the fluidic system in the Aero Commander airplane at 10,000 feet altitude for a commanded heading change of 25° .

Altitude-Hold Mode

Obtaining stable performance for the altitude-hold mode was more difficult than with any of the other fluidic control loops. Initially, the pressure gain was 590 for the pitch damper and 170 for the altitude-error loop. However, the altitude-hold mode was unstable for all altitudes at which it was tested and could not be stabilized by changing gains alone.

As discussed earlier, the altitude-hold mode consists of two feedback signals: pitch rate and an altitude error. The system is mechanized so that engaging the altitude-hold mode engages both feedbacks simultaneously. To analyze the altitude-hold mode, the mode switching was modified to allow operation of the pitch damper with and without the altitude-error feedback. The pitch damper was then evaluated at different altitudes; the flight-test results did not indicate any stability problem in this loop. Efforts were then centered on the altitude-error loop. Futile attempts were made to improve stability by investigating the effects of mechanization changes, relocating the ambient-pressure source, and removing a downspring in the elevator control system. Since the system-lag source could not be found, the altitude lead-lag network was analyzed to determine if additional phase lead could be obtained. Frequency-response tests indicated that the network had a phase lead of 28° instead of its designed 47° . This discrepancy was corrected by component modification. Flight tests with this modification indicated that the stability of the altitude-hold mode was improved at 5000 feet altitude, but not at 10,000 feet altitude. With further adjustment of the system gains, however, stable performance was finally obtained at an altitude of 10,000 feet. The final pressure gains used were 1100 for the pitch damper and 36 for the altitude-error loop. These gains are not suggested as optimum; they are noted only because they did produce a stable flight condition at the altitudes investigated.

The response of the altitude-hold system to a 50-foot step input is shown in figure 17. A maneuver was performed in which the altitude-hold mode was engaged and the pilot physically overpowered the system by moving the control column against the

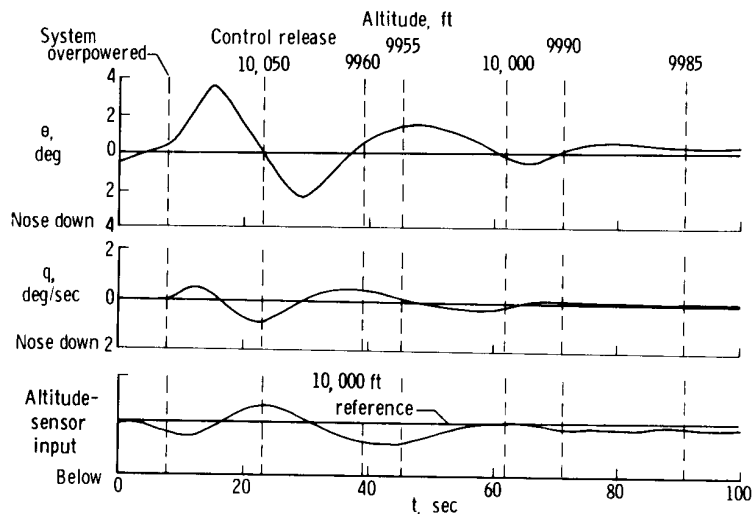


Figure 17.—Altitude-hold-mode response of the fluidic system on the Aero Commander airplane to a 50-foot overpower maneuver at 10,000 feet altitude.

actuator force to cause a 50-foot displacement from the commanded 10,000-foot position. The control column was then released, and the aircraft responses were recorded. Time histories of pitch attitude, pitch rate, and altitude-sensor input are shown for this maneuver. The altitude variations are recorded from pilot callouts and are shown in the figure. As shown, the aircraft returned to the reference altitude in approximately 40 seconds.

The performance of the basic aircraft with the aircraft altitude-hold mode disengaged and engaged is compared in figures 18 and 19, respectively. Figure 18 shows the stick-free altitude-hold capability of the airplane for a trimmed flight condition at 10,060 feet altitude. The time history indicates that the aircraft began to develop a diverging phugoid oscillation with a period of approximately 40 seconds and began to lose altitude gradually.

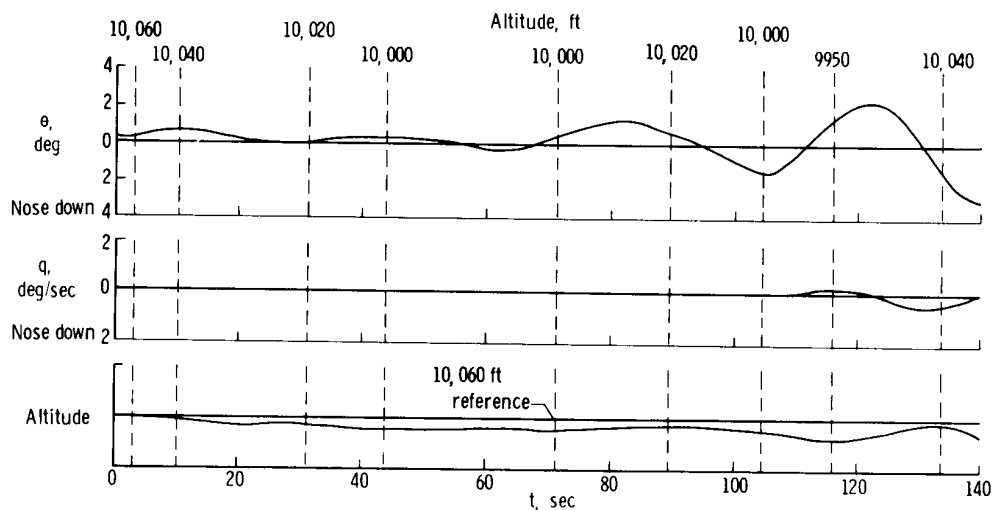


Figure 18.—Stick-free altitude-hold capability of the Aero Commander airplane for trimmed flight at 10,060 feet altitude with the altitude-hold mode disengaged.

The performance of the aircraft retrimmed at 10,060 feet altitude with the altitude-hold mode engaged is shown in figure 19. A slight out-of-trim condition existed when the altitude-hold mode was engaged, which resulted in a pitch transient that produced a 20-foot overshoot above the reference altitude. As can be seen, the transient was damped out by the altitude-hold-mode system, and the oscillations were significantly reduced and stable.

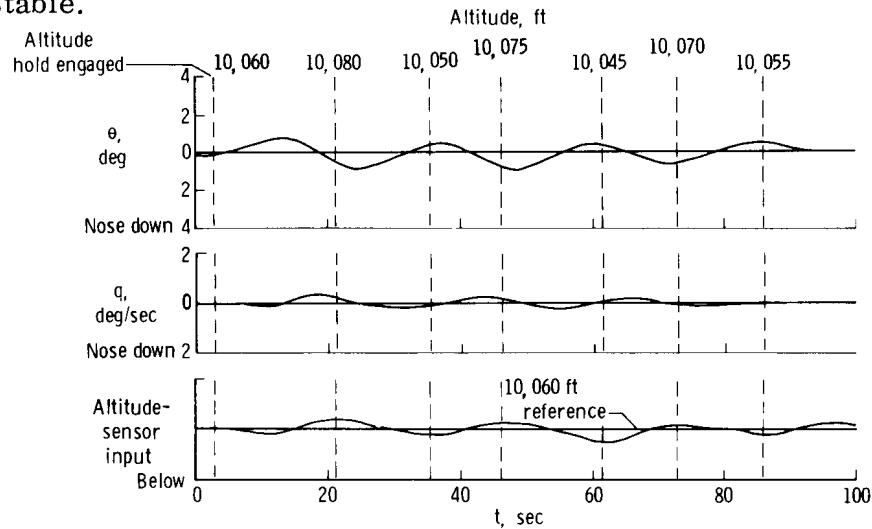


Figure 19. —Altitude-hold performance of the Aero Commander airplane for trimmed flight at 10,060 feet altitude with the altitude-hold mode engaged.

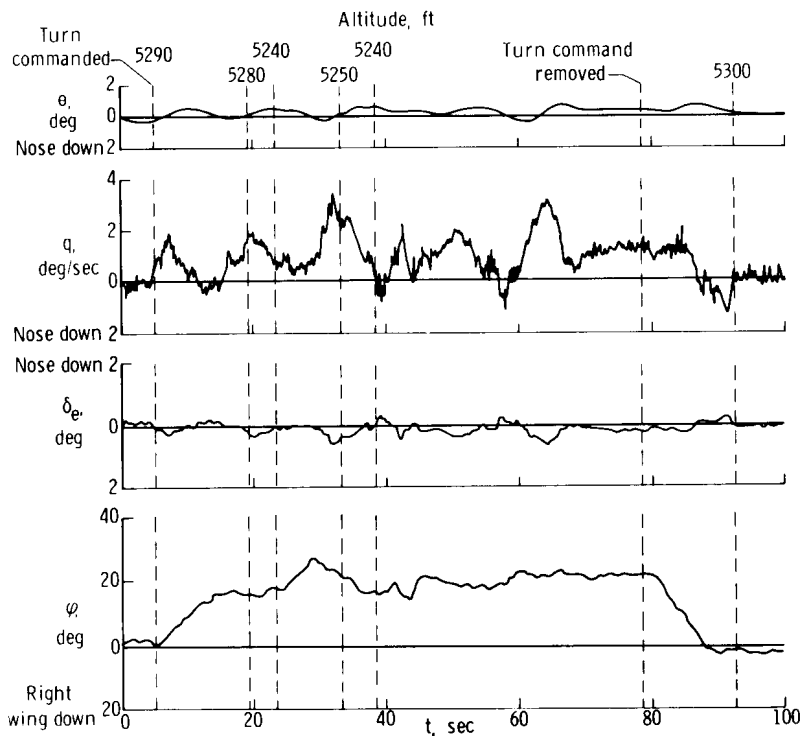


Figure 20. —Turn-command performance of the fluidic system using the wings-leveler mode with the altitude-hold mode engaged at 5300 feet altitude.

Figure 20 is a time history showing the performance of the altitude-hold mode during a commanded left turn using the wings-leveler mode. The wings-leveler and altitude-hold modes were engaged at 5300 feet altitude. The altitude indicated prior to the left turn was 5290 feet, and during the turn a minimum of 5240 feet was observed. The aircraft was returned to the reference altitude after the turn command was removed.

Although stable performance was achieved with this mode of control, additional work is needed to improve the range of the altitude-error sensor and to obtain a linear symmetrical output at the actuator.

PROBLEM AREAS

The large amount of ground and flight-test experience obtained with the fluidic control system uncovered several problems that will require additional work in order to develop a full-time operational system. The characteristics of some of the elements used in the mechanization of the fluidic control system need to be improved in order to reduce nonlinearities and obtain symmetrical outputs.

Trim Control

Considerable difficulty was experienced in obtaining aircraft trim with the fluidic control system. The presence of system-engage transients indicated that the pilot was not able to match system trim with the free-aircraft trim. The amount of mistrim between any axis and its corresponding surface was immediately evident in the magnitude and direction of the engage transient and was particularly noticeable in the longitudinal control mode. These transients were caused by the inability of the pilot to trim each axis because of the location and indication of the fluidic trim devices. The trim circuit used in the fluidic control system does not have a force gradient to represent the trimmed position but relies solely on the positioning of a visual indicator. The indicator does not represent the control-surface trim position relative to the aircraft, but does represent the pressure differential measured across the input to the actuator, which, when zero, represents the control-surface nominal zero position.

To match the system trim with the aircraft trim, the pilot first adjusted the system to correspond with the indicated trim and then engaged the desired axis. If a transient occurred, the pilot disengaged the system and made a small trim correction and then re-engaged the system. This procedure was repeated until the engage transient disappeared. This task, of course, was more difficult when flying in turbulence.

Trim Variance

The fluidic control system trim also appeared to be susceptible to aircraft maneuvers, in that the system trim would change after repeated maneuvers at approximately the same altitude. The out-of-trim condition was particularly noticeable after some of the lateral maneuvers were completed and it became necessary for the pilot to retrim the aileron and rudder control loops. The out-of-trim condition is shown in some of the bank-angle-maneuver data (figs. 7, 8, 12, and 13) by a steady-state bank-angle offset accompanied by some finite yaw rate. The out-of-trim condition was aggravated by relatively high friction forces in the basic aileron control system, which produced a deadband. Flying the fluidic control system in turbulence, however, tended to reduce any apparent system deadband.

System trim change with change in altitude was also observed. The effect of altitude on the overall control-system trim was most noticeable in the lateral axis, particularly when the wings-leveler mode was engaged and trimmed for wings-level flight during a normal climb or descent maneuver. Either periodic trim inputs were required to maintain wings-level flight during the maneuver or the fluidic control system

would gradually cause the airplane to develop an excessive bank angle and increasing yaw rate.

Some of the trim change with altitude can be related to the poor null characteristics of the vortex rate sensor. A pressure transducer was placed across the output of the rate sensor, and the output signal was recorded during flight test. The data indicated that the sensor null changed with changes in altitude. This change in null was reflected throughout the control system as a trim change. These effects indicate that the null characteristics of the vortex rate sensor as well as the fluidic amplifiers need to be stabilized in the presence of pressure variations.

Gain Variance

Altitude effects on the fluidic control system were also observed in the scale factor or gain of the various components. The gain of the vortex rate sensor decreased with increasing altitude, primarily because of the decrease in mass flow through the sensor. Gain losses were also noted in some of the preamplifier stages which used 1.5-psig power supplies. The decrease in gain of the components with increasing altitude caused an overall reduction in the loop gain and could present stability problems with multiloop control systems for some aircraft applications. It will definitely place an altitude limitation on the control system as it was mechanized in this program. To eliminate the altitude effects on closed-loop system gain, it may be necessary to provide a means of scheduling gain as a function of altitude or provide a means to control the environment around the control-system elements.

Pressure Recovery

The pressure recovery of the amplifiers used in the servo network is on the order of 40 percent of the supply pressure. To provide a pressure differential across the input to the actuator of at least 5 psi, the supply pressure of the system was required to be 17.5 psig. The resulting high pressure increased the load on the pneumatic pumps, thus increasing pump temperature and reducing pump life.

Repeatability

The repeatability of the fluidic control system for the same maneuvers was generally good. Some deviation in repeatability was observed during the operation of the heading-select feature of the heading-hold mode, but the basic heading-hold mode appeared to have produced good results.

SYSTEM RELIABILITY

The overall reliability of the fluidic control system was good. Even though the mechanization of the control system was of a breadboard nature, no failures were experienced in any of the sensors or amplifier elements. There were failures in two types of related components—the engine-driven pneumatic pump and the system trim device.

One of the pneumatic pumps failed after 211 hours of flight, of which 28 hours were used for flight investigation of the fluidic control system. The pneumatic exhaust temperature for each pump was monitored throughout the flight-test program. The temperatures for the pump that failed were consistently 5° to 10° higher than normal. However, the exact cause of the failure is unknown.

The fluidic system trim devices failed eight times. All failures were similar in that the spool shaft seized up with the case, thus preventing any additional trim inputs. An improvement in the design of these trim devices would eliminate this problem.

CONCLUDING REMARKS

The results of a flight investigation of a fluidic autopilot system demonstrated that a system of this type can be mechanized for light-aircraft application. Although stability problems were encountered early in the flight program, stable performance was achieved in each control mode for the flight conditions tested. High reliability of the elements with no moving parts was demonstrated. The only system failures were in the mechanical fluidic components.

The data obtained during the flight investigation revealed a number of areas in which improvement is needed before the system can be considered operational. Among these are:

1. The gain of amplifiers and sensors was reduced with increased altitude.
2. The directional gyro used in the mechanization of the heading-hold mode has several undesirable characteristics, such as unsymmetric output and a small linear portion of the overall range of the sensor.
3. The altitude-hold loop needs additional work to obtain a linear symmetrical output from the altitude-error sensor to the servo.
4. The null characteristics of the fluidic components need to be stabilized in the presence of pressure changes associated with changes in altitudes.
5. The low pressure recovery of the present fluidic servo amplifiers dictates high supply pressure and causes loading on the aircraft's pneumatic system.

Flight Research Center,
National Aeronautics and Space Administration,
Edwards, Calif., April 22, 1969,
125-19-03-02-24.

APPENDIX

DESCRIPTION OF THE SYSTEM COMPONENTS

Aircraft Motion Sensors

Four sensors were required to mechanize the fluidic control system: a yaw-rate sensor, a pitch-rate sensor, a directional gyroscope, and an altitude-error sensor.

The rate sensors used in the mechanization of this autopilot are referred to as vortex rate sensors because of the use of a flowing fluid to sense angular rotation. The three basic parts of the vortex rate sensor are the coupling element, the vortex chamber, and the signal pickoff. The coupling element, vortex chamber, and the flow paths of the fluid are shown in figure 21. Flow paths are represented by arrows, which show the fluid entering a plenum chamber and passing through a coupling element into the vortex chamber and toward the center outlet. A "sink" flow field, shown by the radial dashed lines, exists when there is no input turning rate applied to the case. However, when an input turning rate is imparted to the case, its tangential velocity is in turn imparted to the fluid particles as they leave the inside boundary of the coupling element. This tangential velocity superimposed upon the existing radial flow causes the streamlines to assume a logarithmic spiral, which is shown by the solid arrows. As the logarithmic spiral stream flows into the sink outlet, it assumes a helical flow pattern. A pickoff senses the magnitude of the swirl velocity of the fluid, which is proportional to turning rate.

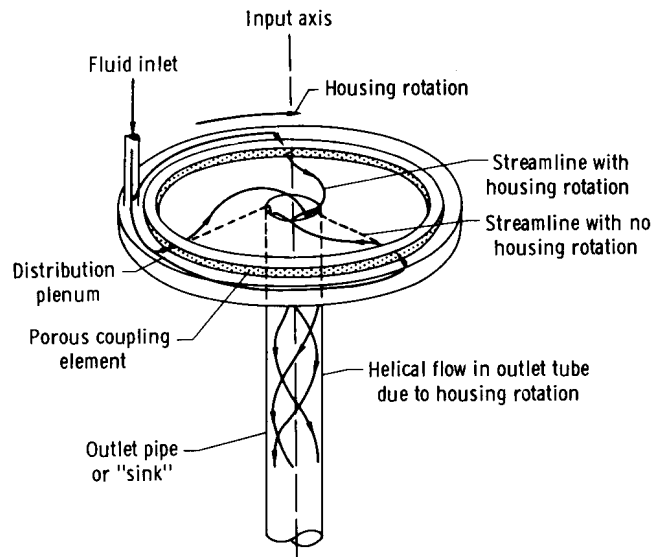


Figure 21.—Vortex-rate-sensor flow phenomenon.

The scale factor of the vortex rate sensor is directly proportional to the mass flow of the fluid through the sensor. (Scale factor is defined as the units of differential pressure per degree per second angular motion.) Two factors, power supply pressure and ambient pressure, then determine the scale factor once the rate-sensor configuration is set. The sensor scale factor is important in that once the sensor scale factor is set and the servoactuator scale factor determined, loop pressure gain is fixed.

Rate-sensor diameter and the operating pressure are key performance tradeoff factors. The diameter of the unit for a given supply pressure determines the sensor threshold and sensor transportation delay time. As the diameter is increased, transportation time is increased and threshold is decreased. The threshold of the rate sensors used on the autopilot is on the order of 0.10 degree per second. The units are approximately 6 inches in diameter and 0.75 inch thick.

The directional gyro is driven pneumatically and has a pneumatic pickoff, as shown schematically in figure 22. The directional-gyro rotor gimbal causes a differential signal pressure proportional to angular displacement up to approximately $\pm 5^\circ$. From $\pm 5^\circ$ to $\pm 15^\circ$ displacement, the signal becomes nonlinear, and beyond $\pm 15^\circ$ the maximum signal pressure is obtained. At 90° of error a phase reversal will occur. A movable stator permits manual selection of heading command.

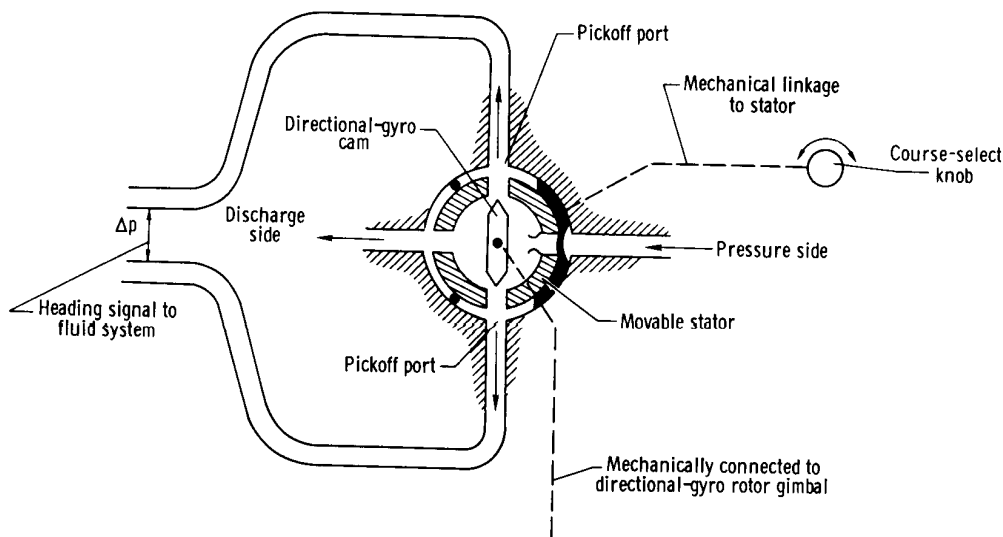


Figure 22.—Diagram of the directional-gyro pneumatic pickoff.

The altitude-error sensor consists of a dual chamber with a mechanical flapper, as shown schematically in figure 23. Both chambers are initially vented to ambient pressure. When altitude hold is commanded, the pressure in one chamber is trapped as a reference. As altitude changes occur, the differential pressure between the two chambers causes the flapper to be deflected accordingly. Flapper movement is used to create a differential signal pressure in proportion to altitude error. Unit threshold is approximately ± 5 feet of altitude.

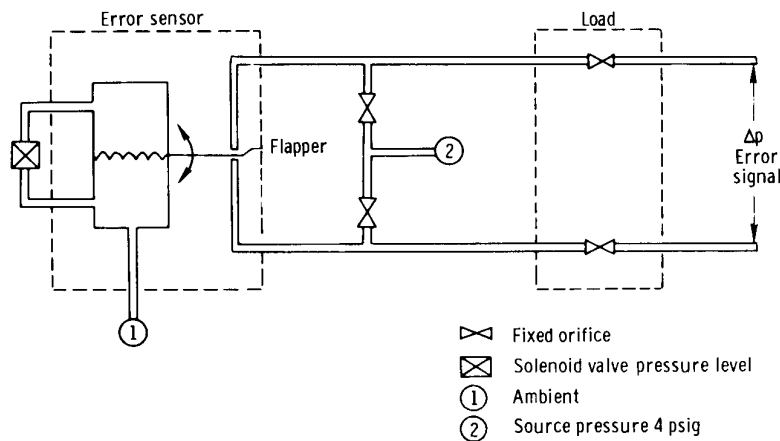


Figure 23.—Schematic drawing of the altitude-error sensor.

Amplifiers and Networks

Vented amplifiers were selected for this system because of the impedance matching difficulty with closed amplifiers. With closed amplifiers, variations in output load affect the input characteristics of the amplifier and are reflected back through each stage of the cascade.

Two types of amplifiers are used in the system: proportional and bistable. All control loops utilize proportional amplifiers from the sensor through the pulse-width-modulator summing stage. Bistable amplifiers are used for the remainder of the loop, including the power amplifier.

The proportional amplifiers selected are of the beam-deflection type. The amplifiers are chemically etched in copper beryllium. Cover plates are brass and contain the necessary connection tubes. The amplifiers are fabricated in several configurations of impedance and number of input or control ports.

Most of the proportional amplifiers used in the system have power ports 0.010 inch wide and 0.005 inch deep, thus providing high-impedance input for the fluidic sensor signals.

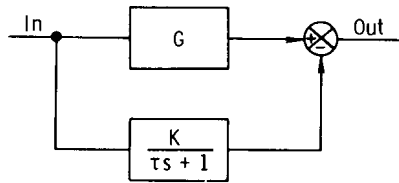
The bistable amplifiers used in the system are aluminum-filled epoxy-cast devices. The power-port width and depth vary from 0.015 inch and 0.020 inch to 0.040 inch and 0.10 inch, respectively. The largest width is used in power amplifiers. The power-amplifier stage consists of two bistable amplifiers in cascade, and the pressure recovery of the amplifiers is on the order of 40 percent. Because of this inefficiency, a high source pressure is required to attain a desired output pressure level. Both pulse-width modulated power-amplifier cascade and analog power-amplifier cascade were considered for this application. Pulse-width modulation was selected primarily because the dither frequency of the pulse-width modulator reduces the servoactuator deadband. The pulse-width cascade is mechanized with bistable amplifiers which have a greater

pressure recovery than proportional amplifiers. Thus, a greater power gain is realized. Both mechanizations result in a proportional control loop and have no effect on the system block diagram.

The design of a cascade requires that certain amplifier characteristics for a set or family of amplifiers be available. The available operating pressures, required pressure gain and control range, and desired gain adjustment must be known before amplifiers can be selected.

The desired loop gain, the sensor scale factor, and the servoactuator transfer function were used to determine the required pressure gain. The required sensor range for each loop was set during the analog-computer simulation.

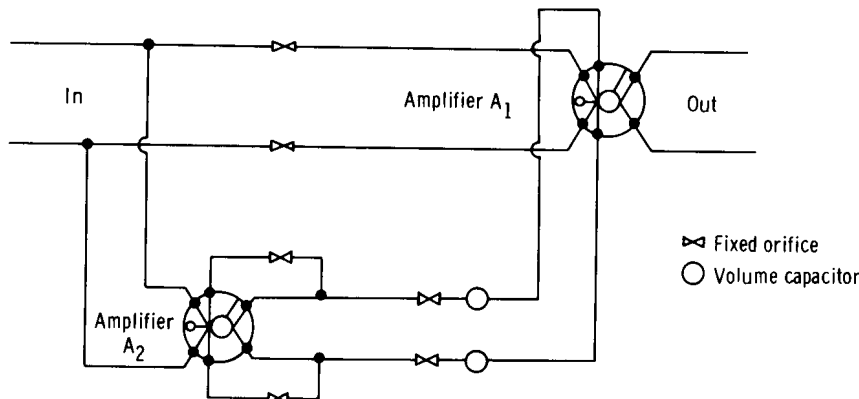
The amplifier operating pressures are 13.5 psig, 4 psig, and 1.5 psig. These values were determined by considering the operating conditions of the amplifiers in terms of Reynolds number and its effect on null shift and pressure gain. Flow ranges for the power nozzle which result in Reynolds numbers associated with transition from laminar to turbulent flow were avoided by proper selection of power supply level. Resistive elements are restrictors, and capacitive elements are volumes. By series and parallel connection of these components with amplifiers, network characteristics can be achieved. Figure 24 shows the mechanization of a high-pass filter. Differential pressure is applied to amplifier A1 and simultaneously to amplifier A2. Under low-frequency, steady-state conditions, the differential input pressure applied directly to



where $G = K$

$$\frac{Out}{In}(s) = \frac{G\tau s}{1 + \tau s}$$

(a) System block diagram.



(b) Fluid network schematic.

Figure 24. -Mechanization of a high-pass network.

amplifier A1 is canceled by the output pressure of amplifier A2; thus, the output pressure of amplifier A1 is at a null. The response to a higher frequency input is such that the signal is passed directly to the output of amplifier A1 because of the attenuation and lag by way of amplifier A2.

In addition to the high-pass network, other networks such as lead-lag and pulse-width modulators are mechanized in the system.

Surface Servoactuators

Off-the-shelf pneumatic actuators were modified to satisfy the servo requirement. The area of the cylinder was chosen by considering the input pressure and the required output force. Stroke was set by the cable travel needed. The modified unit retained its proved overpower mechanism and method of attachment to the airframe and control cables. The servoactuators consist of two cylinders with pistons sealed against pressure loss by rolling diaphragms, as shown in figure 25. The piston rods drive against an output linkage which is designed to transfer the linear motion of the rod to torque on a control-system cable drum. Differential pressure applied to the input ports of the actuator causes one piston to extend and the other to retract. When the servo is disengaged, the cylinders are vented to the atmosphere. A spring-loaded pivot on the output linkage permits the pilot to overpower the system.

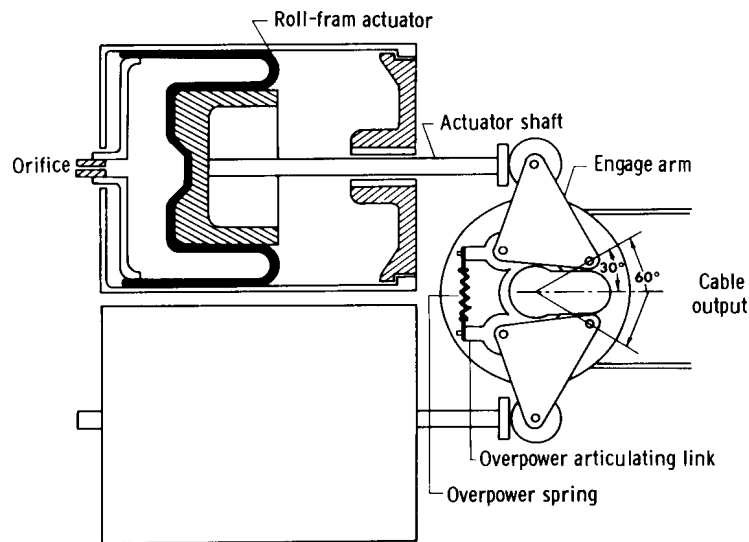


Figure 25.—Schematic drawing of servoactuator.

Parallel connection of the force-limited surface actuators was anticipated, since it was desirable for the pilot to be aware at all times of control-system inputs. Three actuators were required: aileron, elevator, and rudder. These actuators are torque-limited and use no position feedback.

Control-Loop Mechanization

The longitudinal-axis mechanization is shown in the schematic drawing of figure 26. This loop contains a rate sensor and preamplifier, an altitude-error sensor and shaping network, summing amplifier, pulse-width modulator, power amplifier, and actuator. The pilot can command altitude hold and has a manual pitch-trim control.

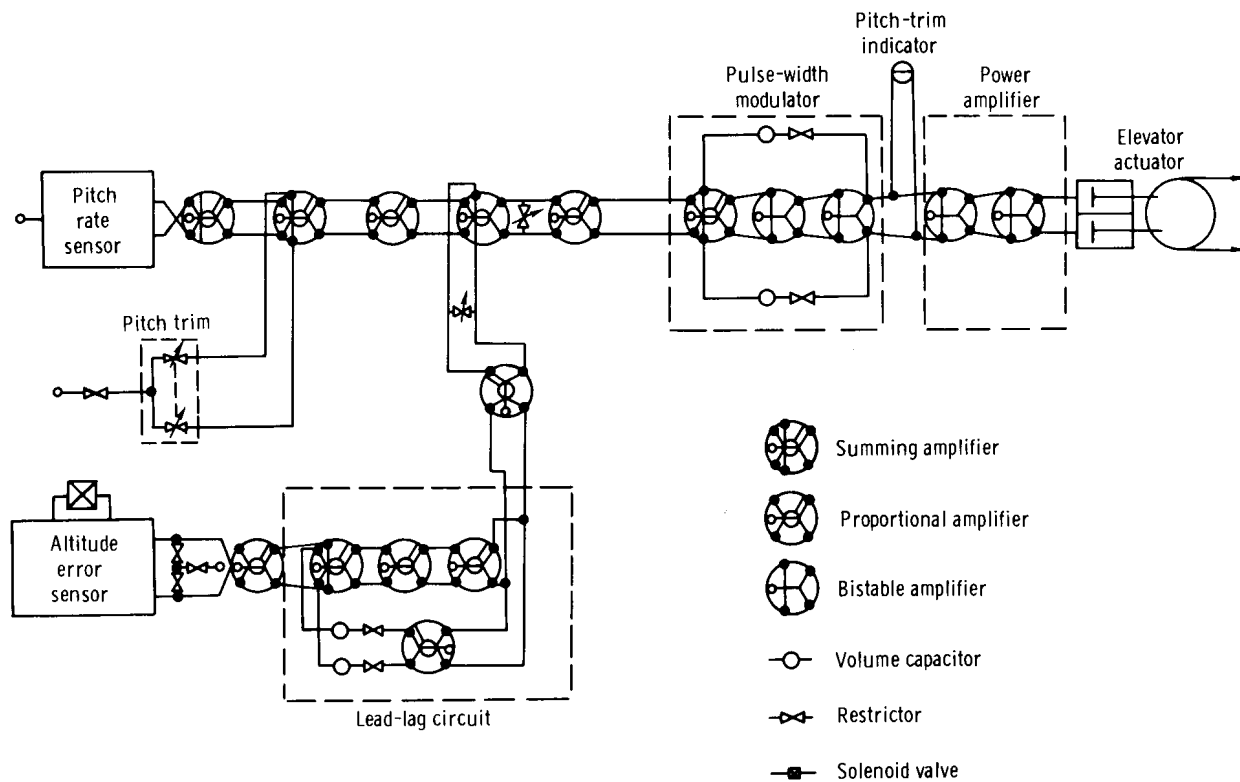


Figure 26.—Schematic drawing of the longitudinal-axis mechanization.

A schematic drawing of the mechanization of the lateral-directional axes is shown in figure 27. The yaw-damper loop contains a rate sensor, preamplifier, high-pass filter, pulse-width modulator, power amplifier, and actuator. Yaw rate and aircraft heading are summed as the control input to the roll axis (wings leveler). The heading loop is mechanized the same as the yaw-damper loop except that the heading loop has more summing amplifiers and no high-pass network.

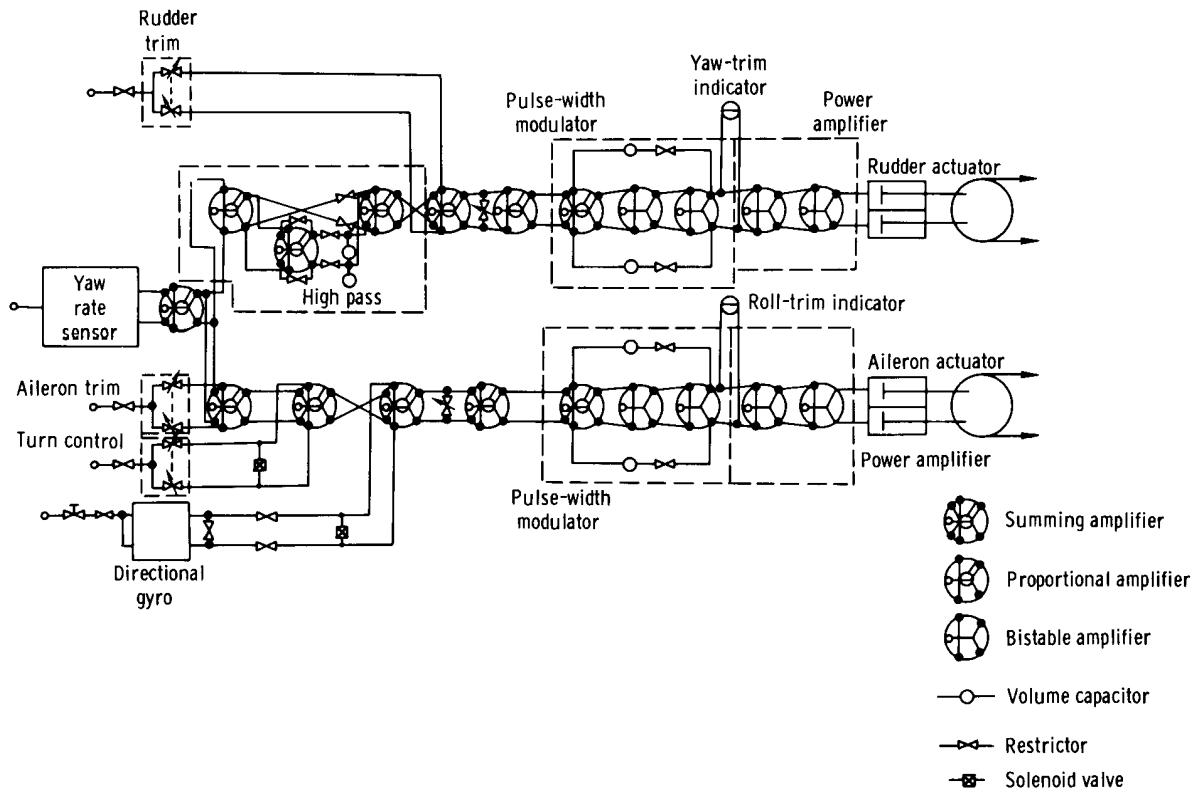


Figure 27.—Schematic drawing of the lateral-directional-axes mechanization.

REFERENCES

1. Fluid Flight Systems Section: Study of Fluid Flight Path Control System. Honeywell Inc. (NASA CR-758), 1967.
2. Rodgers, D. L. : Development and Flight Testing of a Fluidic Flight Control System. Honeywell Inc. (NASA CR-913), 1967.
3. Lock, Wilton P. ; Gee, Shu W. ; and Rodgers, Daniel L. : Design, Development, and Flight Testing of a Pure Fluid Autopilot. NASA paper presented at SAE Committee A-6 Symposium on Fluidics, San Francisco, Calif. , Oct. 21, 1966.